doi:10.17596/0003759

白鳳丸研究航海報告

＊ 航海番号　　ＫＨ-２２-６次研究航海

＊ 航海名称　　日本海溝海側における海洋プレート上層部での水の流動と熱輸送過程の研究
Study of fluid flow and heat transport processes in the uppermost part of the Pacific plate on the seaward side of the Japan Trench

＊ 観測海域　　日本海溝～北西太平洋
Japan Trench and northwest Pacific areas

＊ 航海期間　　令和４年４月６日（水）～令和４年４月２２日（金）

＊ 出港日時・場所　４月　６日１３時３０分　東京港

＊ 入港日時・場所　４月２２日１１時　　東京港

＊ 寄港期間・場所　なし

＊ 研究課題　　日本海溝海側における海洋プレート上層部での水の流動と熱輸送過程の研究

＊ 主席研究員（氏名・所属・職名）
山野　誠・東京大学地震研究所・教授

＊ 研究内容，主調査者，観測項目
１．地殻熱流量測定による、海洋地殻内の流体循環と熱輸送過程の研究
山野　誠、熱流量プローブ及びピストンコアラーによる熱流量測定

２．堆積物・間隙水試料採取による、断層近傍での流体流動の研究
鹿児島　渉悟、ピストンコアラー及びマルチプルコアラーによる堆積物および海底直上水の採取

３．エアロゾル採取による、大気沈降物質の研究
　　張　勁、エアーサンプラーによるエアロゾル採取

４．地磁気異常の観測による、海洋地殻構造の研究
　　後藤　忠徳、船上三成分磁力計による磁場測定

５．海底地形探査による、火山体の研究
　　平野　直人、マルチビーム音響測深装置（MBES）による地形・底質調査

６．地層探査による、地質構造の研究
　　川村　喜一郎、地層探査装置（SBP）による地質構造調査

＊ 乗船研究者氏名・所属・職名
　　山野　誠　・東京大学地震研究所・教授
　　木下　正高・東京大学地震研究所・教授
　　藤田　親亮・東京大学地震研究所・技術専門職員
　　芦田　将成・東京大学大気海洋研究所・技術職員
　　張　勁　　・富山大学学術研究部理学系・教授
　　鹿児島渉悟・富山大学学術研究部理学系・特命助教
　　野口　忠輝・富山大学大学院理工学教育部・大学院生
　　鄧　文傑　・富山大学大学院理工学教育部・大学院生
　　大塚　進平・富山大学大学院理工学教育部・大学院生
　　遠藤　真樹・富山大学理学部・学部生
　　後藤　忠徳・兵庫県立大学大学院生命理学研究科・教授
　　池田　尚史・山口大学大学院 創成科学研究科・大学院生
　　股村　祐希・東北大学大学院 理学研究科・大学院生
　　横川真一朗・マリン・ワーク・ジャパン海洋地球科学部・観測技術員
　　小松　亮介・MOL マリン海洋事業室・観測技術員

＊ 航跡・測点図

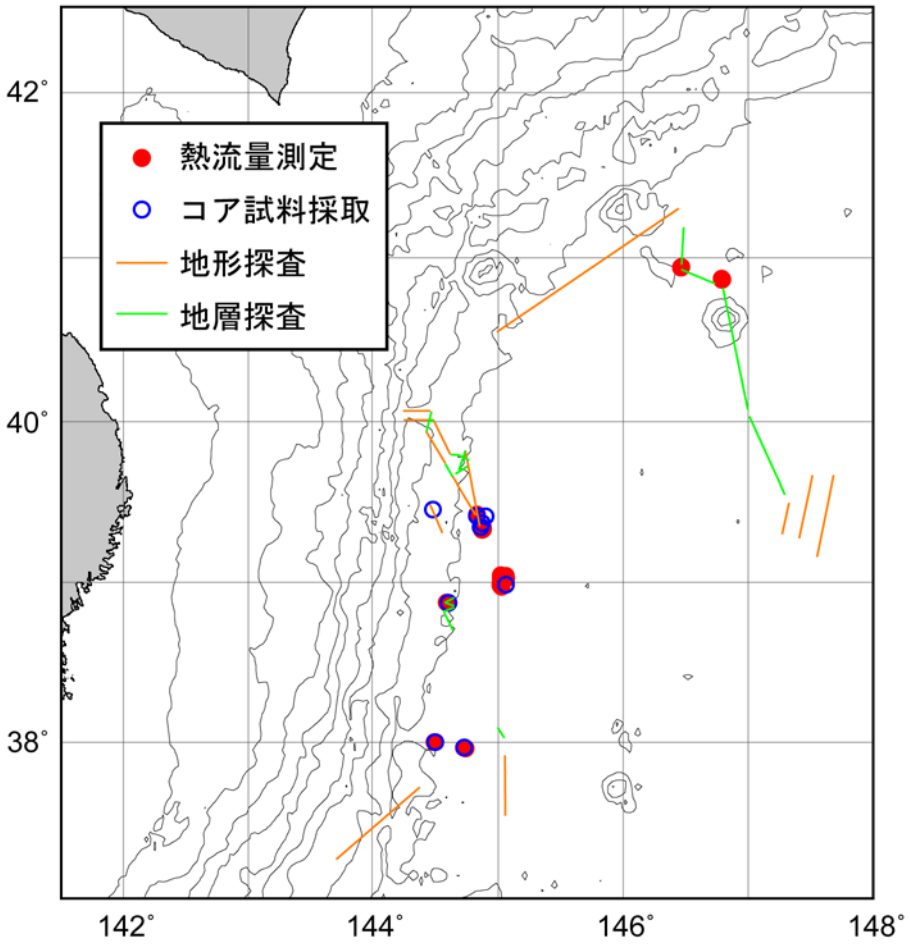

Contents

1. Cruise Information

Cruise ID:

KH-22-6

Name of vessel:

R/V HAKUHO MARU

Title of cruise:

Study of fluid flow and heat transport processes in the uppermost part of the Pacific plate on the seaward side of the Japan Trench

Chief scientist:

Makoto YAMANO Earthquake Research Institute, The University of Tokyo

Cruise period:

April 6, 2022 – April 22, 2022

Ports of departure / arrival:

2022 April 6 Dept. from Tokyo

April 22 Arriv. at Tokyo

Research area:

Japan Trench and northwest Pacific areas

Research map:

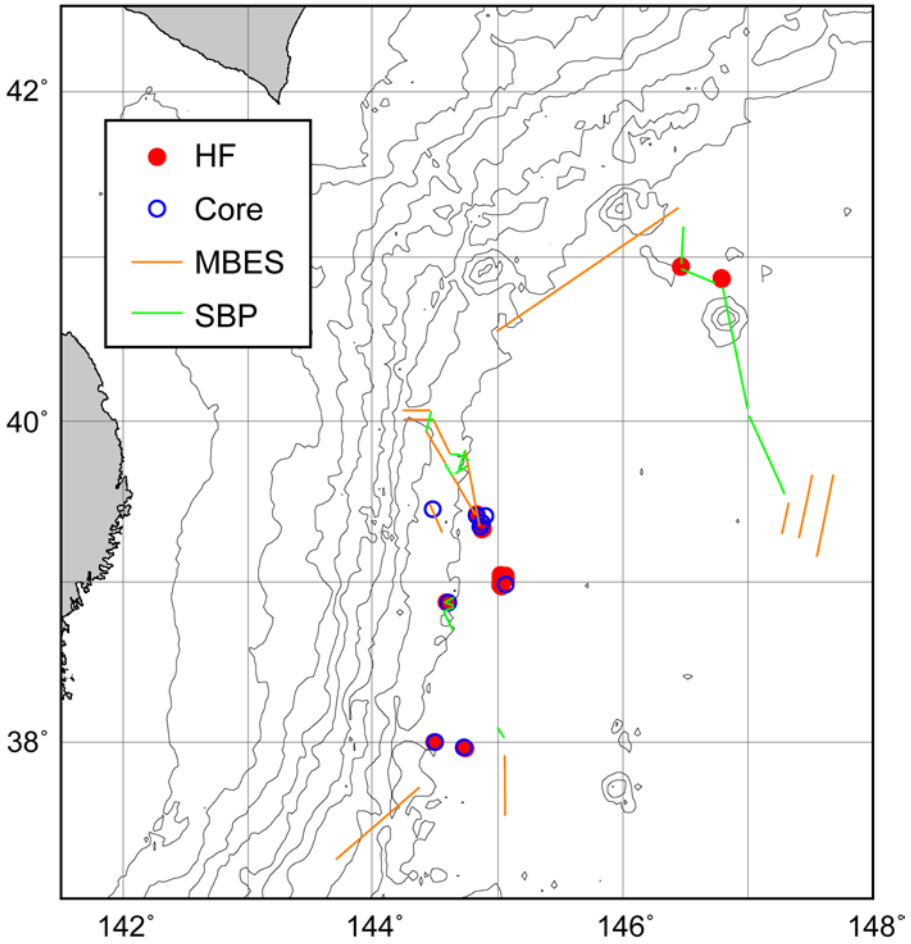

Figure 1-1. Locations of observation points and survey lines.
HF: heat flow measurement, Core: sediment core sampling, MBES: multi-beam echo-sounder survey, SBP: sub-bottom profiling survey

2. Research Proposal and Science Party

Title of proposal:

Study of fluid flow and heat transport processes in the uppermost part of the Pacific plate on the seaward side of the Japan Trench

Representative of science party:

Makoto YAMANO	Earthquake Research Institute, The University of Tokyo

Science Party:

Makoto YAMANO	Earthquake Research Institute, The University of Tokyo
Masataka KINOSHITA	Earthquake Research Institute, The University of Tokyo
Chikaaki FUJITA	Earthquake Research Institute, The University of Tokyo
Masanari ASHIDA	Atmosphere and Ocean Research Institute, The University of Tokyo
Jing ZHANG	Faculty of Science, Academic Assembly, University of Toyama
Takanori KAGOSHIMA	Faculty of Science, Academic Assembly, University of Toyama
Tadateru NOGUCHI	Graduate School of Science and Engineering for Education, University of Toyama
DENG Wenjie	Graduate School of Science and Engineering for Education, University of Toyama
Shinpei OTSUKA	Graduate School of Science and Engineering for Education, University of Toyama
Masaki ENDO	School of Science, University of Toyama
Tada-nori GOTO	Graduate School of Science, University of Hyogo
Yuki MATAMURA	Graduate School of Science, Tohoku University
Hisashi IKEDA	Graduate School of Science and Technology for Innovation, Yamaguchi University
Jin-Oh PARK	Atmosphere and Ocean Research Institute, The University of Tokyo (shore-based)
Asuka YAMAGUCHI	Atmosphere and Ocean Research Institute, The University of Tokyo (shore-based)
Kiichiro KAWAMURA	Graduate School of Sciences and Technology for Innovation, Yamaguchi University (shore-based)
Naoto HIRANO	Center for Northeast Asian Studies, Tohoku University (shore-based)
Shiki MACHIDA	Ocean Resources Research Center for Next Generation, Chiba Institute of Technology (shore-based)
Hiroshi ICHIHARA	Graduate School of Environmental Studies, Nagoya University (shore-based)

Tomohiro TOKI	Faculty of Science, University of the Ryukyus (shore-based)
Takafumi KASAYA	Japan Agency for Marine-Earth Science and Technology (shore-based)
Gou FUJIE	Japan Agency for Marine-Earth Science and Technology (shore-based)
Yoshifumi KAWADA	Japan Agency for Marine-Earth Science and Technology (shore-based)
Shusaku GOTO	Geological Survey of Japan, National Institute of Advanced Industrial Science and Technology (shore-based)

Technical Support Staff

Shinichiro YOKOGAWA	Marine Works Japan, Ltd.
Ryosuke KOMATSU	MOL Marine Co., Ltd.

3. Research Activities

3.1. Research Objectives

Recent surveys made on the seaward side of the Japan Trench revealed various features indicating flows of fluid, material and heat in the upper most part of the incoming Pacific plate: petit-spot volcanism, a broad high heat flow zone, and anomalies in the seismic velocity structure (e.g., Hirano et al., 2006; Yamano et al., 2014; Fujie et al., 2018). Such flows should change the physical/chemical conditions of the subducting plate, the input to the subduction zone, which is a very important factor in studies on subduction zones. We therefore planned comprehensive research of fluid and heat flow processes in the trench outer rise area in cooperation with wide fields of earth science and have been conducting it supported by a JSPS KAKENHI (Grant Number 18H03733).

This cruise (R/V HAKUHO MARU KH-22-6) was proposed as a major component of the above-mentioned research project. We investigate fluid flow along normal faults developed on the seaward slope of the Japan Trench through concentrated heat flow measurements and analysis of pore water and gas extracted from sediment samples. Heat flow measurements are made on the outer rise of the Japan and Kuril trenches as well to reveal characteristics of the heat flow distribution, which may reflect pore fluid circulation and heat transport processes resulting from fracturing of the oceanic crust. We also conduct multi-beam echo-sounder and sub-bottom profiler surveys for investigation of petit-spot volcanism and contourite drifts. Multi-channel seismic reflection survey around normal faults, which is a part of the same research cruise proposal, will be conducted on another HAKUHO MARU cruise KH-22-9 in November 2022.

3.2. Cruise Schedule and Operations

Date	Events, Operations
April 6	Leave Tokyo Transit to the survey area (Japan Trench and NW Pacific areas)
April 7	Arrive in the survey area MBES test survey Heat flow measurement (HF01)
April 8	MBES test survey Heat flow measurement (HF02)
April 9	Heat flow measurement (HF02, continued) Core sampling with heat flow measurement (HFPC01) SBP and MBES survey
April 10	SBP and MBES survey (continued) Core sampling (MC01) Core sampling with heat flow measurement (HFPC02) Heat flow measurement (HF03)
April 11	Heat flow measurement (HF03, continued) Core sampling (MC02) Core sampling (PC03) Heat flow measurement (HF04)
April 12	Heat flow measurement (HF04, continued) Core sampling with heat flow measurement (HFPC04) Heat flow measurement (HF05)
April 13	Heat flow measurement (HF05, continued) Core sampling with heat flow measurement (HFPC05) MBES survey
April 14	MBES survey (continued) Heat flow measurement (HF06) Heat flow measurement (HF07)
April 15	Heat flow measurement (HF07, continued) MBES survey Take refuge from rough sea (off Hachinohe)
April 16	Take refuge from rough sea (off Hachinohe)
April 17	Transit to the survey area
April 18	Arrive in the survey area Heat flow measurement (HF09)
April 19	Heat flow measurement (HF09, continued) Core sampling (MC03) Core sampling with heat flow measurement (HFPC06) Heat flow measurement (HF10)
April 20	SBP and MBES survey Core sampling with heat flow measurement (HFPC07) Core sampling with heat flow measurement (HFPC08) Heat flow measurement (HF11)
April 21	Heat flow measurement (HF11, continued) Leave the survey area
April 22	Arrive at Tokyo

3.3. Research Activities

3.3.1. Heat flow measurement

1) Background and objectives

Anomalous heat flow values, higher than that expected for the seafloor age of the incoming Pacific plate, are pervasively distributed on the outer rise of the Japan Trench (Yamano et al., 2014). Overlapping the broad anomaly, local variations at a scale of several kilometers were detected through concentrated measurements along lines perpendicular to the trench. The broad high heat flow zone seaward of the trench can be attributed to pore fluid circulation in a permeable layer developed through fracturing of the oceanic crust due to plate bending, which efficiently pumps up heat from deeper part of the crust (Kawada et al., 2014). Local variations may have arisen from heterogeneous development of fractures: higher surface heat flow is observed at sites where the crust has been fractured down to deeper part.

On the seaward slope of the Japan Trench, where normal faults are well developed, heat flow data had been sparse compared to dense data on the outer rise. Measurements made around faults with large surface displacement on recent cruises (KS-15-16 and KS-16-15 cruises of the R/V SHINSEI MARU and KH-20-8 cruise of the R/V HAKUHO MARU) showed that heat flow distribution around the faults may have different features from those of on the outer rise. On this cruise, we conduct concentrated measurements in the vicinities of several faults for investigation of influence of normal faults on fluid flow and heat transport processes in the incoming oceanic crust.

We conducted heat flow measurements on the seaward side of the Kuril Trench off Hokkaido in 2018 on the KH-18-5 cruise of the R/V HAKUHO MARU. Heat flow on the Kuril Trench outer rise was found to be generally normal for the seafloor age, in contrast to the high anomaly off the Japan Trench. To examine this feature in more detail, additional measurements are made on this cruise.

2) Measurement method

Heat flow is obtained as the product of the geothermal gradient and the thermal conductivity. We measured the geothermal gradient by penetrating an ordinary deep-sea heat flow probe or a heat flow piston coring system (HFPC) into seafloor sediments.

[Instruments]

The deep-sea heat flow probe (Fig. 3.3-1) weighs about 800 kg and has a 3.0 m-long lance, along which seven compact temperature recorders (Miniaturized Temperature Data Logger, ANTARES Datensysteme GmbH; Fig. 3.3-2) are mounted in an outrigger fashion (Ewing type). A heat flow data logger (Kaiyo Denshi Co., DHF-650) placed inside the weight head (cf. Fig. 3.3-4) was used for recording the tilt and the depth of the probe. Tilt and depth data were sent to the surface with acoustic pulses so that we can monitor the status of the probe on the ship.

Temperature profiles in surface sediment were measured with a piston corer as well. For this

purpose, we used a core head specially designed for mounting the heat flow data logger, and temperature recorders (MTLs) were attached along the 4-m or 6-m long core barrel (Fig. 3.3-3). We call this system the heat flow piston coring system (HFPC).

Figure 3.3-1. Deep-sea heat flow probe.

Figure 3.3-2. ANTARES Miniaturized Temperature Data Logger (MTL).

Figure 3.3-3. Heat flow piston coring system (HFPC) with temperature data loggers (MTLs).

[Operations]

A 20-m long nylon rope was inserted between the heat flow probe and the winch wire rope in order not to kink the wire rope during probe penetrations. An acoustic transponder was attached about 100 m above the probe for precise determination of the position of the probe (Fig. 3.3-4).

Multi-penetration heat-flow measurement operations were conducted following the procedures described below.

1. Measure water temperature about 30 m above the seafloor for calibration of the temperature recorders.
2. Lower the probe at a speed of about 1 m/sec until it penetrates into the sediment.
3. Measure temperatures in the sediment for about 15 min. Monitor the wire tension and pay out the wire when necessary to keep the probe stable.
4. Pull out the probe.
5. Move to the next station keeping the probe about 100 m above the seafloor.
6. Repeat penetrations.

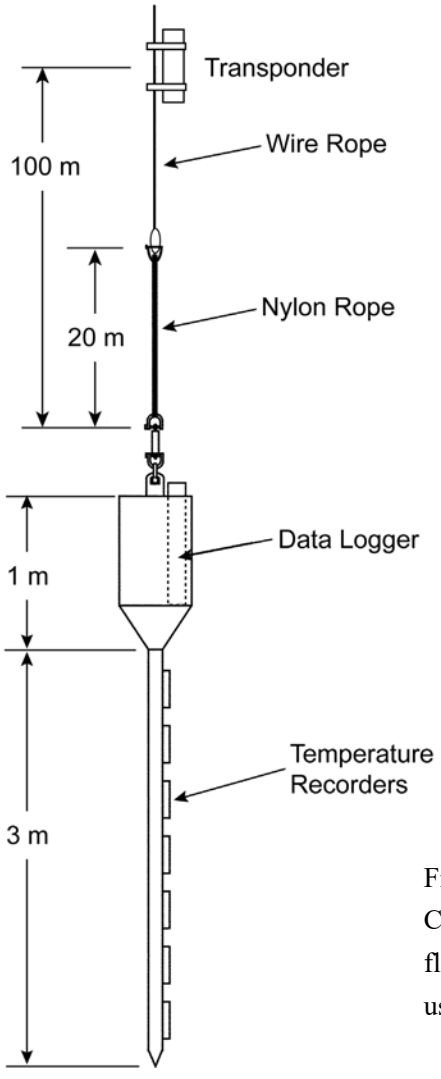

Figure 3.3-4. Configuration of the heat flow measurement system using a deep-sea probe.

The operation procedure for the HFPC is similar to that for ordinary piston coring system, except the HFPC is kept on the seafloor for about 15 min. for measurement of temperature distribution in sediment. The 20-m long nylon rope was used for the HFPC as well.

3) Preliminary results

We carried out heat flow measurements in three areas: 1) in the vicinities of normal faults developed on the seaward slope of the Japan Trench, 2) along short N-S lines on the Japan Trench outer rise (around 39°N, 145°E), 3) on the outer rise of the Kuril Trench around 41°N, 146.5°E,. Most of the measurements were made with the deep-sea heat flow probe at intervals of 300 to 500 m to detect local variations. At seven core sampling sites (HFPC01, 02, and 04 through 08), the heat flow piston coring system (HFPC) was used.

We attempted 93 penetrations in total and 56 of them were successful (Table 3.3-1). Most of the coordinates of the measurement points in Table 3.3-1 are the positions of the acoustic transponder determined with the SSBL system of the ship. At some stations, the listed coordinates are those estimated from the ship's position since the positions of the transponder were not well determined. The water depth in the table is the depth measured by the heat flow data logger.

Measurements in the vicinities of normal faults were made at four sites: HF02, HFPC01, 02 and 05 around 39.4°N, HF03 around 39.3°N, HF10 and HFPC06 around 38.9°N, HF11 and HFPC08 around 38.0°N. Two of them (HF02 and HFPC01, 02 and 05; HF11 and HFPC08) are very close to sites where anomalously high $^{3}He/^{4}He$ ratios were found in pore water of surface sediment (Park et al., 2021, cf. 3.3.4). We also made measurements at a reference site (HF01 and HFPC07), about 20 km east of HF11 and HFPC08, where normal faults have not been well developed.

On the Japan Trench outer rise around 39°N, previous concentrated survey along an E-W line normal to the trench showed prominent heat flow variations at a scale of 3 to 5 km. We have been conducting dense measurements along two N-S lines as well to examine heat flow variation in the trench-parallel direction. At HF04, 05, and 09, we made measurements to extend heat flow profiles along the N-S lines.

Heat flow measurements on the Kuril Trench outer rise were conducted at two sites (HF06 and 07) off the easternmost part of Hokkaido. First detailed measurements in this area were made in 2018 and no high values for the seafloor age were obtained. For further investigation of characteristics in the heat flow distribution off the Kuril Trench, we made additional measurements in the same area.

Heat flow values will be obtained by combining the measured temperature profiles with thermal conductivity of surface sediment. Thermal conductivity needs to be estimated from the values measured on piston core samples and the existing data on the Japan and Kuril trench outer rises.

Table 3.3-1. Results of heat flow measurements

Date	Station	Latitude (N)	Longitude (E)	Depth (m)	N
Deep-sea heat flow probe					
April 7	HF01A	37°57.66'	144°44.20'	5550	5
	B	37°57.78'	144°43.99'	5555	6
	C	37°57.87'	144°43.71'	5555	6
	D	37°57.93'	144°43.48'	5560 5	6
April 8	HF02A	39°24.92'	144°49.54'	5805	fell
	B	39°24.92'	144°49.52'	5805	fell
	C	39°24.94'	144°49.53'	5805	fell
	D	39°25.17'	144°49.58'	5805	3
	E	39°25.34'	144°49.58'	5815	fell
	F	39°25.35'	144°49.59'	5815	fell
	G	39°25.41'	144°49.48'	5810	fell
	H	39°25.42'	144°49.48'	5810	fell
	I	39°25.42'	144°49.47'	5810	fell
April 9	J	39°25.43'	144°49.47'	5810	fell
	K	39°25.50'*	144°49.43'*	5805	fell
	L	39°24.50'*	144°49.43'*	5805	fell
	M	39°25.67'	144°49.46'	5805	fell
	N	39°25.67'	144°49.46'	5810	fell
	O	39°25.72'	144°49.62'	5810	fell
	P	39°25.73'	144°49.65'	5810	6
April 10	HF03A	39°20.83'	144°52.52'	5690	2
	B	39°20.68'	144°52.52'	5690	2
	C	39°20.44'	144°52.55'	5700	2
	D	39°20.25'	144°52.56'	5700	2
	E	39°20.14'	144°52.32'	5705	4
April 11	F	39°20.09'	144°52.19'	5710	4
	G	39°20.06'	144°52.11'	5705	4
	H	39°20.04'	144°52.10'	5705	4
	HF04A	39°02.82'	145°03.54'	5530	5
April 12	B	39°02.64'	145°03.58'	5535	6
	C	39°02.44'	145°03.59'	5535	5
	D	39°02.23'	145°03.62'	5535	4
	E	39°02.00'	145°03.63'	5535	4
	F	39°01.75'	145°03.66'	5530	3
	G	39°01.52'	145°03.67'	5525	fell
	H	39°01.49'	145°03.68'	5525	fell
April 12	HF05A	39°03.02'	145°01.12'	5510	3
	B	39°02.91'	145°01.18'	5510	4
	C	39°02.71'	145°01.18'	5515	4
	D	39°02.47	145°01.17'	5515	4
	E	39°02.20'	145°01.15'	5520	4
	F	39°01.96'	145°01.13'	5525	4
April 13	G	39°01.68'	145°01.15'	5535	4
	H	39°01.42'	145°01.14'	5540	fell
	I	39°01.40	145°01.15'	5540	fell
	J	39°01.38'	145°01.15'	5540	fell
	K	39°01.18'	145°01.15'	5540	4

		L	39°01.13'	145°01.16'	5540	4
	April 14	HF06A	40°52.10'	146°47.21'	5210	7
		B	40°52.14'	146°47.40'	5210	7
		C	40°52.34'	146°47.23'	5205	6
		D	40°52.46'	146°47.13'	5205	7
		HF07A	40°56.49'	146°27.55'	5255	6
		B	40°56.67'	146°27.65'	5260	6
		C	40°56.75'	146°27.75'	5260	6
	April 18	HF09A	38°59.56'	145°00.98'	5535	fell
		B	38°59.56'	145°00.96'	5535	fell
		C	38°59.58'	145°00.95'	5535	6
		D	38°59.57'	145°00.93'	5535	fell
		E	38°59.56'	145°00.92'	5535	fell
		F	38°59.56'	145°00.92'	5535	fell
		G	38°59.23'	145°00.92'	5535	6
		H	38°59.01'	145°00.94'	5530	fell
		I	38°58.97'	145°00.95'	5530	fell
		J	38°58.95'	145°00.94'	5530	fell
		K	38°58.89'	145°00.96'	5525	fell
		L	38°58.86'	145°00.96'	5525	fell
		M	38°58.82'	145°00.98'	5525	fell
		N	38°58.74'	145°01.47'	5525	fell
		O	38°58.73'	145°01.51'	5525	6
		P	38°58.62'	145°01.58'	5525	fell
		Q	38°58.61'	145°01.58'	5525	fell
	April 19	R	38°58.59'	145°01.58'	5525	fell
		HF10A	38°52.66'	144°36.07'	6270	6
		B	38°52.71'	144°35.87'	6265	6
		C	38°52.71'	144°35.78'	6260	fell
		D	38°52.73'	144°35.72'	6255	6
		E	38°52.75'	144°35.54'	6130	5
		F	38°52.76'	144°35.30'	6050	5
		G	38°52.78'	144°35.14'	6015	6
	April 20	HF10A	38°00.04'	144°29.68'	6025	4
		B	38°00.05'	144°29.55'	6030	7
		C	38°00.05'*	144°29.45'*	6025	7
	April 21	D	38°00.04'	144°29.35'	5970	fell
		E	38°00.04'	144°29.33'	5955	fell
		F	38°00.05'	144°29.28'	5945	6
HFPC						
	April 9	HFPC01	39°25.22'	144°49.62'	5785	4
	April 10	HFPC02	39°25.06'	144°53.84'	5615	4
	April 12	HFPC04	38°59.50'	145°03.58'	5470	6
	April 13	HFPC05	39°25.04'	144°53.81'	5620	6
	April 19	HFPC06	38°52.69'	144°35.90'	6205	5
	April 20	HFPC07	37°58.00'	144°43.61'	5525	1
		HFPC08	38°00.03'	144°29.62'	6000	4

N: number of temperature sensors used to obtain temperature profile in sediment.

*: estimated based on the ship's position.

4) Thermal conductivity measurement

Thermal conductivity of sediment core samples was measured using two different types of line-source commercial devices. One is QTM-700 (Kyoto Electronics Manufacturing Co.) with a half-space type box probe (Sass et al., 1984). The other is KD2 Pro Thermal Properties Analyzer (Decagon Devices, Inc.) with a full-space type needle probe (von Herzen and Maxwell, 1959). KD2 Pro has the ability to measure thermal diffusivity (or heat capacity) as well as thermal conductivity by using dual-needle sensors (dual probes; Bristow et al., 1994), while measurements with ordinary single-needle sensors (single probes) give thermal conductivity only. We conducted measurements with these devices on split core samples.

3.3.2. Sediment core samples

We collected sediment core samples at eight sites using piston corers with 4-m or 6-m long core barrels (HFPC01, 02, PC03, HFPC04 through 08; Table 3.3-2). A 1-m long gravity corer with a liner tube of 75-mm diameter was used as the pilot corer. Photographs and visual descriptions of the split core samples are shown in Fig. 3.3-5. It should be noted that some parts of the samples are not shown because they were removed as whole-round samples for pore-fluid analysis.

Undisturbed surface sediment samples were taken at three sites with a multiple corer (MC01, 02 and 03; Table 3.3-2).

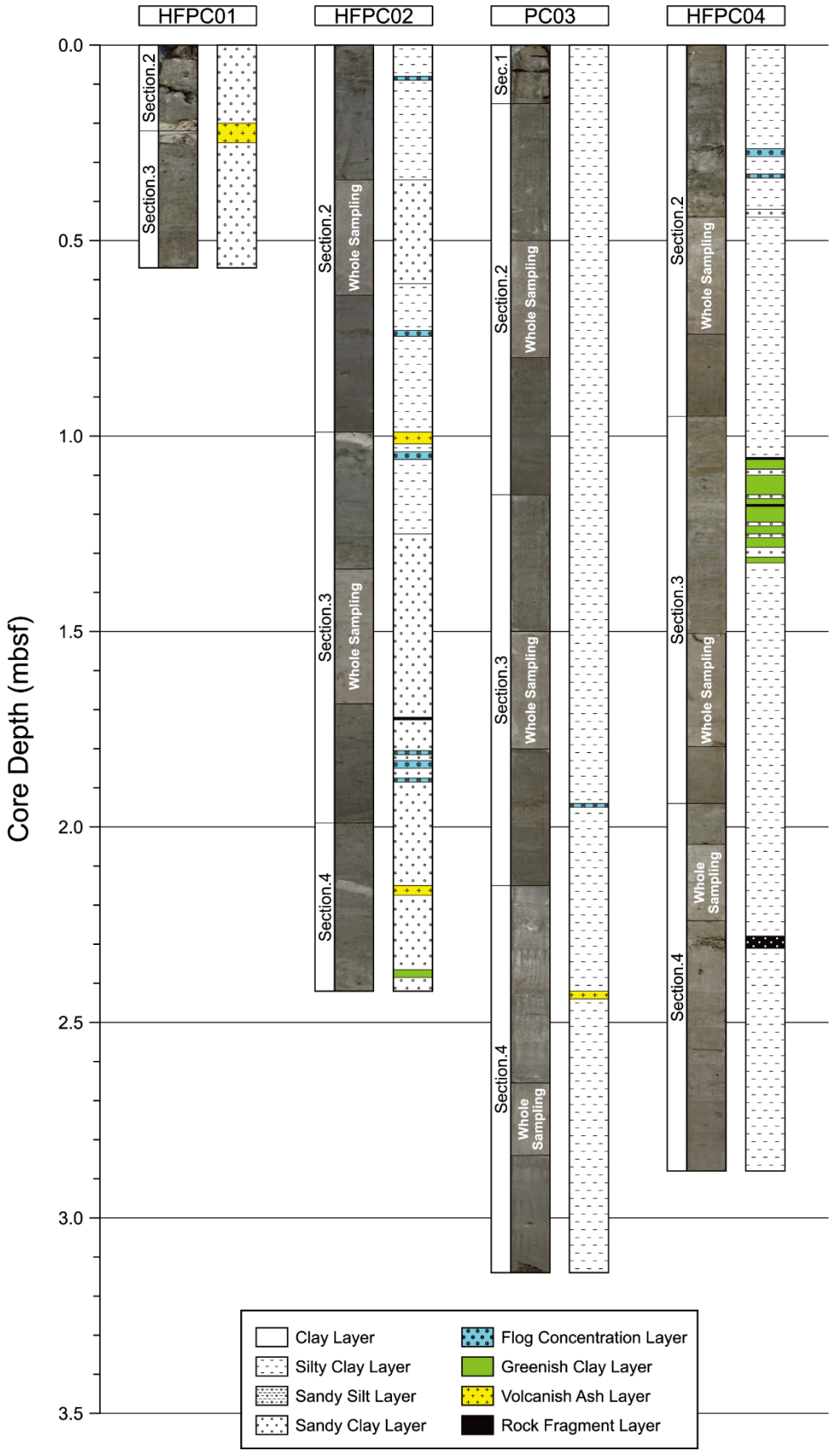

Figure 3.3-5. Photos and visual descriptions of piston core samples.

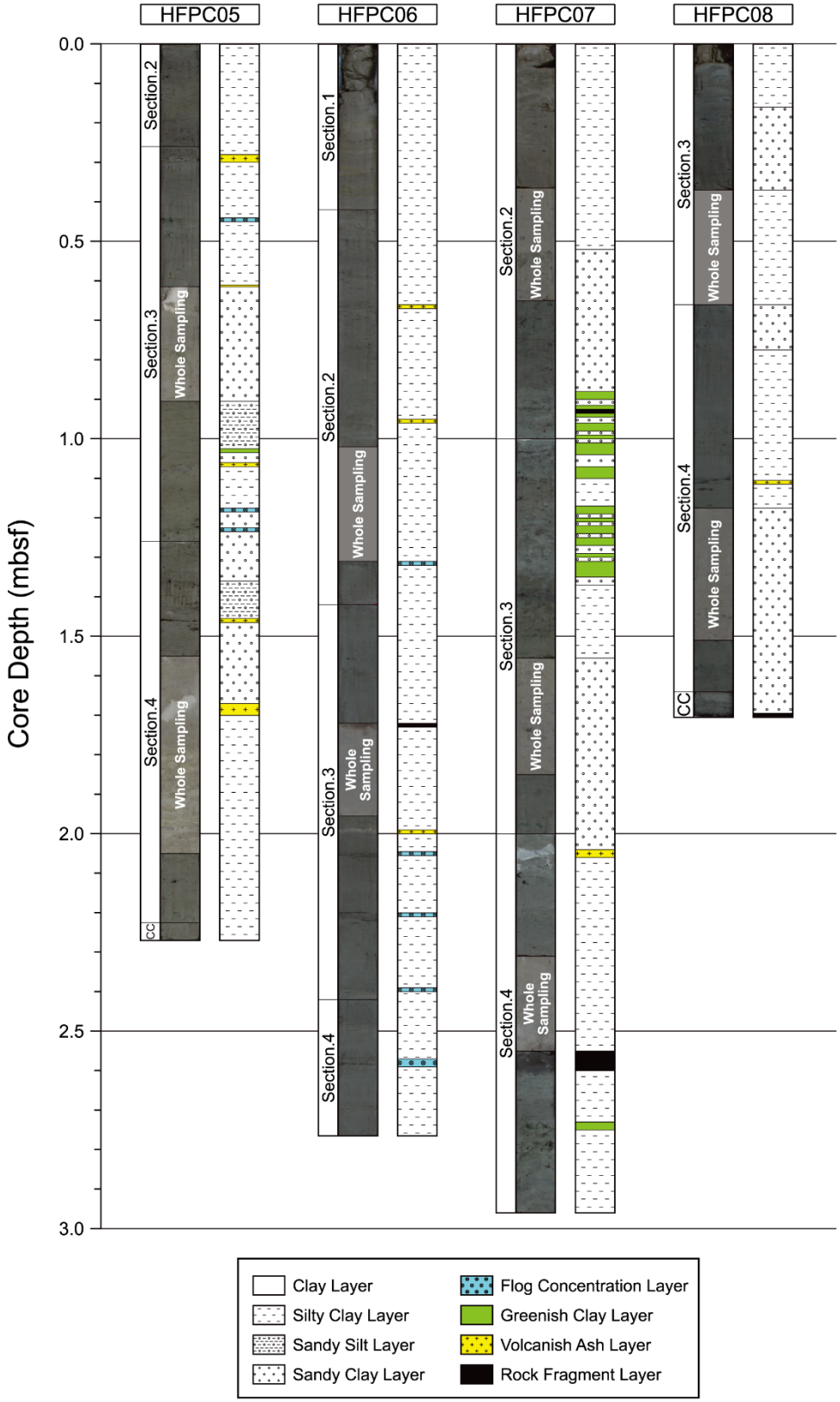

Figure 3.3-5. (continued)

3.3.3. Interstitial water geochemistry (1) major elements

1) Background

In the Japan Trench-Outer Rise region, previous studies have suggested the existence of fluid circulation along faults. It is believed that water captured by the oceanic plate can be ultimately transported to the Earth's interior, which can affect the water distribution and temperature structure, and even further affect the seismic activity. Hence, it is extremely important to clarify the details of fluid circulation beneath the seafloor in the trench-Outer rise region. In this study, sediments and pore water samples will be collected on the seaward side of the Japan Trench, especially near faults, and be analyzed for chemical composition and isotopes. We will also compare the data with those obtained in the same area by the KH-20-8 cruise of the R/V HAKUHO MARU to elucidate the fluid circulation.

2) Sample collection and future plans

During the KH-22-6 cruise of the R/V HAKUHO MARU, we obtained sediments at 8 sites in the Japan trench-Outer rise region (Fig. 3.3-6) using a piston corer (AORI, 500 to 900kg weight) with 4 m or 6 m PVC pipe core tubes and a multiple corer (AORI, 450 kg weight) with eight 60 cm polycarbonate core tubes. Seawater was sampled just above the seafloor using a Niskin-bottle attached to the multiple corer. The coring sites were determined immediately before core collection according to the onboard topographic surveys. PC (piston corer) and PL (pilot corer) samples were cut into 1-m long sections on deck after recovery and were immediately reserved in a cold room (about 4°C). After magnetic susceptibility measurement and whole-round sampling for noble gas analyses, the cores were cut in half within 24 hours then the sediment samples were taken at intervals of 5 cm. MC (multiple corer) samples were kept in a cold room (about 4°C) immediately after recovery, and sediment samples were collected by slicing the cores into 1~3 cm intervals within 24 hours. All the samples were kept in a cold room (about 4°C) during the cruise.

Porewater in the sediments was squeezed at approximately 10 cm intervals for PC and at about 3 cm intervals for MC. This work was performed in the cold room (about 4°C) using syringes and vises (Fig. 3.3-7). The collected porewater was divided into the corresponding containers of each analysis items and stored in an appropriate way. After disembarkation, the nutrient concentrations, major chemical compositions, and oxygen and hydrogen isotope ratios of porewater will be analyzed in the laboratory. These data will be further compared to data acquired on the KH-20-8 cruise.

Table 3.3-2. Sediment sampling stations

Station	Latitude	Longitude	Depth	Date
B-2 (HFPC01)	39°25.22’ N	144°49.62’ E	5810m	2022/4/9 00:11 UTC
B-4 (HFPC02)	39°25.06’ N	144°53.84’ E	5636m	2022/4/10 02:34 UTC
B-1 (PC03)	39°27.57’ N	144°28.59’ E	6800m	2022/4/11 06:25 UTC
B-10 (HFPC04)	38°59.50’ N	145°03.58’ E	5508m	2022/4/12 02:33 UTC
B-4 (HFPC05)	39°25.04’ N	144°53.81’ E	5636m	2022/4/13 01:33 UTC
B-6 (HFPC06 and PL06)	38°52.69’ N	144°35.90’ E	6262m	2022/4/19 01:52 UTC
C-5 (HFPC07 and PL07)	37°58.00’ N	144°43.61’ E	5545m	2022/4/20 01:08 UTC
C-4 (HFPC08 and PL08)	38°00.03’ N	144°29.62’ E	5997m	2022/4/20 07:00 UTC
B-3 (MC01)	39°21.08’ N	144°51.39’ E	5611m	2022/4/9 21:24 UTC
B-3 (MC02)	39°22.47’ N	144°52.11’ E	5614m	2022/4/10 22:45 UTC
B-6 (MC03)	38°52.64’ N	144°35.97’ E	6270m	2022/4/18 21:10 UTC

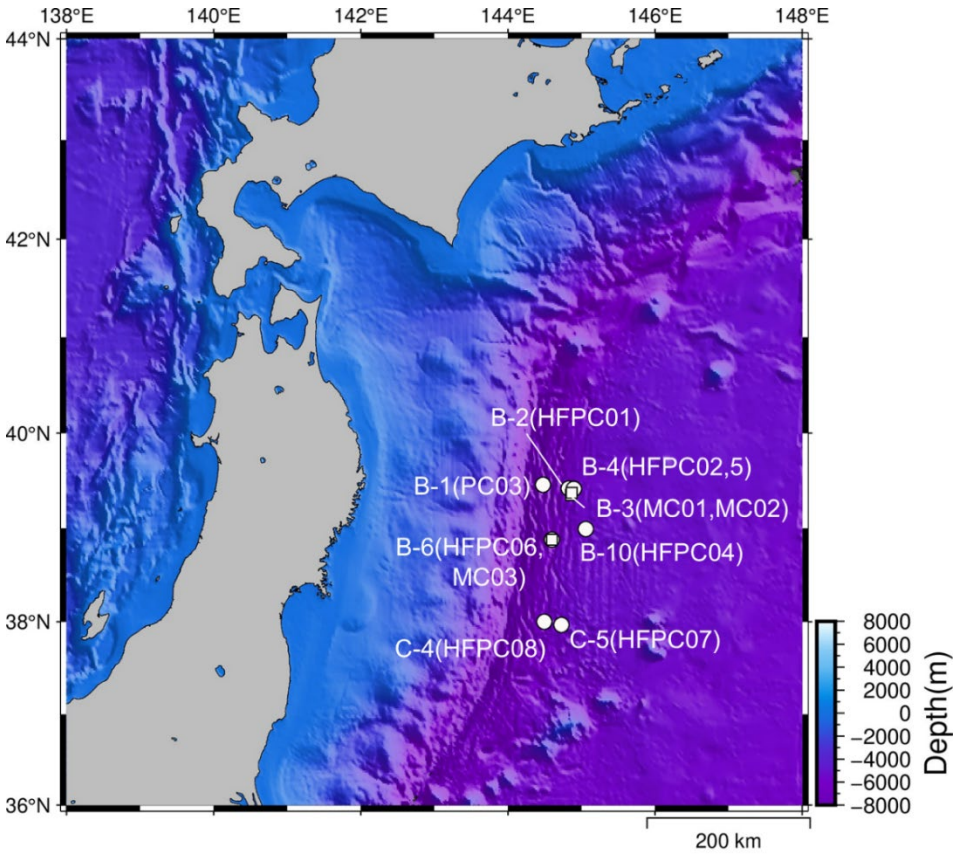

Figure 3.3-6. Location of multiple-corer (MC) and piston-corer (PC) stations in the Japan Trench-Outer Rise region.

Figure 3.3-7. Porewater sampling by using vises.

3.3.4. Interstitial water geochemistry (2) volatile elements

1) Background and purpose

Geochemical characteristics and behavior of pore fluids may be strongly related to tectonic settings and physical phenomena at convergent plate boundaries such as fault-bending and great earthquakes. Isotopic compositions of volatile elements in pore fluids provide crucial information reflecting fluid origins and cycles. For example, helium-3 is one of the most useful tracers for fluid behavior because of its chemical inertness and high sensitivity of mantle-derived components. In this study, isotopic compositions of volatile elements such as noble gases in porewater will be analyzed in order to investigate origins and cycles of fluids around faults which may affect subduction processes as fluid pathways between ocean and the interior of the Earth.

2) Activity: Sediment and seawater sampling

Sediment and seawater samples were collected at stations B-1, B-2, B-3, B-4, B-6, B-10, C-4 and C-5.

3) Methods

Sediment samples were collected using the heat flow piston corer system (HFPC) and the multiple corer system (MC). After HFPC cores arriving on the deck, they were cut and divided into one-meter sections. In addition, one-meter sections were cut and divided into three sections, and the middle 30 to 50-cm cores were used for sediment sampling in order to avoid contamination from edges of the sections. After covering both ends of the 30 to 50-cm cores, their walls were drilled for making holes. Then the copper tubes were connected to the holes in order to transfer sediment into the tubes by squeezing using a jack. For MC sampling, the liner made of acrylic (60-cm long) with through holes on the wall was used. The holes were sealed during core recovering. After core arriving on the deck, copper tubes were connected to the holes in order to transfer sediment into the tubes by squeezing using a jack. Immediately after squeezing, both ends of the copper tubes were sealed by metal clamps in order to avoid air contamination. Seawater samples were collected using a Niskin water sampling bottle mounted on the metal frame of MC. The bottle was equipped with a triggering system using a weight which closes the bottle at two meters above the seafloor. On land, porewater will be extracted from the sediment by centrifugation, and dissolved gases will be extracted from porewater and seawater samples. After purification of the gases, chemical and isotopic compositions of volatiles such as noble gases will be measured.

3.3.5. Multi-beam echo-sounder (MBES) survey

1) Purposes

The first purpose of MBES (multi-beam echo-sounder) survey was to investigate possible petit-spot sites east of the off Tohoku Region. Fujie et al. (2020) showed that petit-spot sites correspond to shallow acoustic basement areas by seismic survey. The eastern part of the survey area of this cruise has other shallow acoustic basement areas, where it is still unclear whether there are petit-spots or not. In this MBES survey, we observed the shallow acoustic basement areas to confirm the presence of a small knoll and high acoustic backscattering strength similar to a petit-spot volcano.

The second purpose was to check the quality of MBES data. R/V HAKUHO MARU is equipped with a new MBES system, EM124 (Kongsberg). We surveyed the same line as the one surveyed on previous cruises to compare the MBES data qualities. And we changed the MBES recording parameter to check the effect of the parameter.

2) Specifications of the MBES system

The specifications of EM124 are shown in Table.3.3-3. Equipment pictures and dataflow are shown in Fig.3.3-8. SeaPath merges GNSS (two modules) and Gyro data and sends it to EM124 Processing Unit (PU). PU controls TX and RX units by order from the SIS user terminal. PU merges SeaPath data and bathymetric data. And PU sends to the user terminal (SIS). SIS makes MBES raw data from PU merged data, surface sound velocity sensor data and user set sound velocity profile.

Table 3.3-3. Specifications of EM124

Feature	Specification
Beamwidths	2°×2°
Number of transmitters	24
Number of receivers	8
Operating frequency	10.5 – 13.5 [kHz]
Swath width	<=150°
Depth range	20 – 11,000 [m]
Number of receiver beams (per ping)	1024（High resolution mode, dual swath）
Sounding pattern	Equidistant and equiangular
Pulse forms	CW and FM chirp
Pulse length	1 – 100 [ms]
Realtime motion stabilization	Roll (±15°), Pitch(±10°), Yaw(±10°)

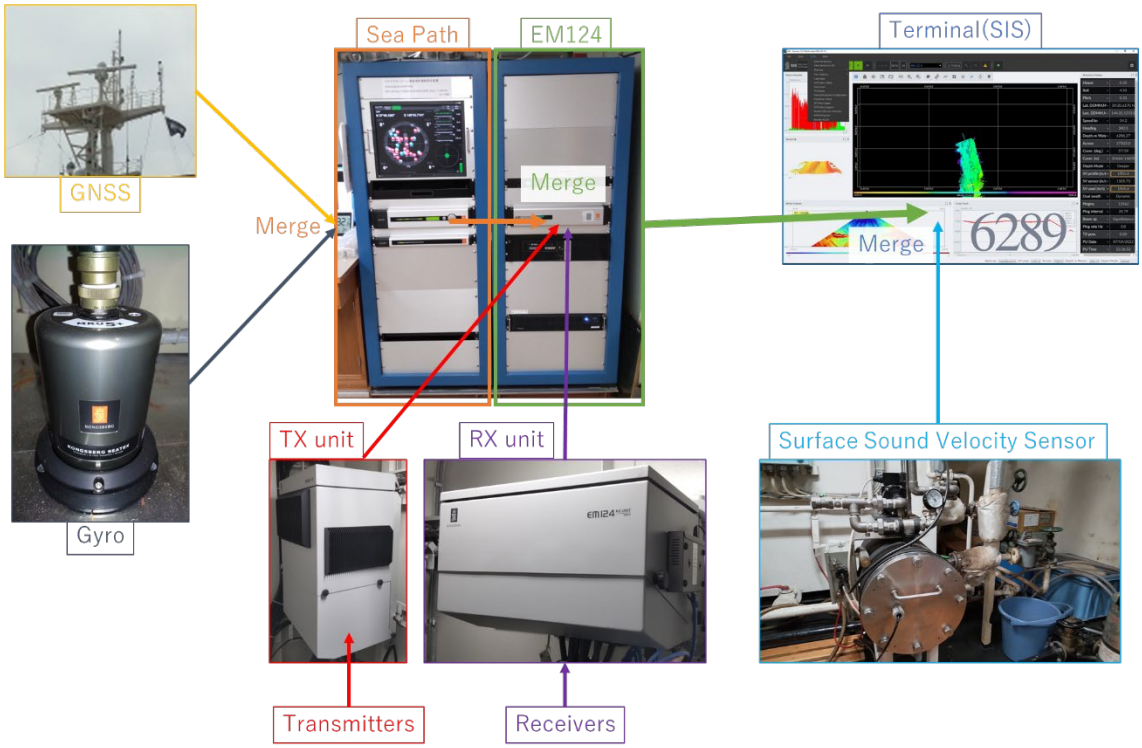

Figure 3.3-8. Equipment and dataflow of Kongsberg EM124

Table 3.3-4. MBES survey lines

No.	In		Out	
	Latitude (N)	Longitude (E)	Latitude (N)	Longitude (E)
EM124 test survey	37°15.22'	143°42.56'	37°42.78'	144°22.59'
EM124 test survey	39°29.40'	144°27.74'	39°18.38'	144°33.78'
	39°18.83'	144°33.78'	39°29.40'	144°27.74'
Area B west survey	39°25.47'	144°49.40'	39°39.77'	144°38.44'
	39°44.42'	144°35.07'	39°56.29'	144°25.87'
	40°03.83'	144°28.08'	40°03.83'	144°14.95'
	40°00.50'	144°15.04'	40°00.50	144°29.54'
	40°00.44'	144°29.61'	39°47.90'	144°37.33'
	39°49.26'	144°44.36'	39°21.40'	144°51.51'
Area B east survey	39°09.81'	147°32.66'	39°40.10'	147°40.96'
	39°40.05'	147°30.70'	39°16.63'	147°24.28'
	39°18.28'	147°15.93'	39°29.98'	147°19.21'
Area A survey	41°17.92'	146°26.87'	40°32.88'	144°59.88'
Area C survey	37°54.96'	145°03.70'	37°31.98'	145°03.69'

3) XBT/XCTD measurement

The time of the XBT/XCTD launch is shown in Table 3.3-5. The time of applying sound velocity profile is shown in Table 3.3-6.

Table 3.3-5. The time of the XBT/XCTD launch

No	Date (JST)	Time (JST)	Type	Length (m)	Lat (D:M)	Lon (D:M)
1	2022/04/07	14:01	XBT (T-5)	1830	37:49.9157	144:33.2228
2	2022/04/18	08:11	XBT (T-5)	1830	39:15.4551	144:33.1818
3	2022/04/10	00:54	XCTD (XCTD-4)	1850	39:50.3968	144:44.7880
4	2022/04/13	21:36	XCTD (XCTD-4)	1850	39:09.4525	147:29.3533
5	2022/0415	04:12	XCTD (XCTD-4)	1850	41:16.9932	146:28.4448
6	2022/04/20	02:16	XCTD (XCTD-4)	1850	38:01.0482	145:03.4361
7	2022/04/20	05:17	XCTD (XCTD-4)	1850	47:31.5726	145:03.1724

Table 3.3-6. The time of applying sound velocity profile

No	Date (JST)	Time (JST)	Data
1	2022/04/07	14:23	1st XBT+Levitas
2	2022/04/08	08:32	2nd XBT+Levitas
3	2022/04/10	01:23	3rd XCTD+Levitas
4	2022/04/13	21:59	4th XCTD+Levitas
5	2022/04/15	04:37	5th XCTD+Levitas
6	2022/04/17	22:06	1st XBT+Levitas
7	2022/04/20	02:35	6th XCTD+Levitas

3.3.6. Sub-bottom profiler (SBP) survey

The Japan Trench is one of active convergent margins with a convergence rate of ca. 8 cm/yr, where the Pacific plate subducts beneath the Honshu Arc (the North American plate). The Pacific plate on the outer slope of the Japan and Kuril trenches is characterized by horst-graben structures, seamounts, petit-spot volcanoes, and outer rise with a rough bathymetry. Along the outer slope of the Japan and Kuril Trenches, we observe northward strong bottom currents originating from the Lower Circumpolar Deep Water (LCDW) flow in the Antarctic Ocean (Ando et al., 2013). The rough bathymetry could make small isolated contourite drifts. The deposition of these drifts could be shifted with local redirection of the flow axis of the bottom currents. To identify and to survey in detail the contourite drifts, we conducted SBP (sub-bottom profiler) surveys on elevated and mounded bathymetry indicating isolated drifts (Table 3.3-7).

Table 3.3-7. SBP survey lines

Line No.	In		Out	
	Latitude (N)	Longitude (E)	Latitude (N)	Longitude (E)
BS1_NS1	38°42.2'	144°38.9'	38°49.1'	144°34.5'
BS1_EW2	38°49.7'	144°34.5'	38°50.9'	144°39.4'
BS1_EW3	38°51.5'	144°39.4'	38°52.8'	144°34.5'
BS1_EW4	38°52.8'	144°34.5'	38°54.6'	144°39.3'
BS2_NS1	38°39.8'	144°38.4'	39°44.4'	144°35.1'
BS3_NS1	39°56.3'	144°25.9'	40°03.8'	144°28.1'
BS3_EW2	40°00.5'	144°26.9'	40°00.5'	144°29.5'
BS4_EW1	39°47.9'	144°37.3'	39°47.7'	144°41.6'
BS4_EW2	39°47.7'	144°41.6'	39°45.6'	144°46.5'
BS4_EW3	39°43.6'	144°45.6'	39°40.8'	144°40.0'
BS4_NS4	39°42.0'	144°41.2'	39°49.3'	144°44.3'
AS5_NS1	41°11.6'	146°29.2'	40°57.6'	146°28.3'
AS5_NS2	40°56.0'	146°27.9'	40°50.8'	146°44.3'
AS5_NS3	40°49.3'	146°48.0'	40°04.6'	147°00.0'
AS5_NS4	40°02.0'	147°01.0'	39°33.1'	147°17.8'
CS6_EW1	38°05.8'	145°00.0'	38°01.6'	145°03.3'

3.3.7. Magnetic field measurement

Bending of the incoming oceanic plate on the seaward side of the Japan Trench should cause various processes in the oceanic crust such as fracturing, faulting, and alteration due to fluid circulation. The geomagnetic field measured in the outer rise area may include information on these processes, which cause variations of the structure and magnetization of the oceanic crust.

Three components of the geomagnetic field were measured with STCM (shipboard three component magnetometer) throughout the cruise. For estimation of the influence of the magnetic field produced by the ship, we made measurements while turning the ship's heading by 360 degrees at three different latitudes. The obtained data will be analyzed in combination with other geophysical data, e.g., bathymetry and gravity.

3.3.8. Aerosol and surface water sampling

1) Background and purpose

To accurately assess the origin and composition of seafloor sediments and stromal waters, it is necessary to distinguish between atmospheric dry deposition, advection from coastal, and landslides. Seafloor sediments are composed of atmospheric dry deposition, as well as inflows from the coast, horizontal advection from other waters, and biological activity by living organisms. In order to understand the contribution of each source to the composition of sea floor sediments, we observed the atmospheric dry deposition in addition to direct sampling and measurement of sea floor sediment. We believe this makes it possible to define the characteristics of the Kuril Trench and its surrounding environment from the viewpoint of material transportation. Furthermore, we expect to be able to capture seasonal and interannual changes by comparing samples obtained during a cruise in 2020 (KH-20-8) to those obtained during this cruise in the same area.

In this cruise we have collected aerosol samples to understand the effects of atmospheric deposition on seafloor sediments. We also have collected samples for Chl-a, Cells Counting that are useful in assessing the contribution of aerosol to surface ocean primary production and the impact of primary production on seafloor sediments.

2) Sampling methods

Aerosol:

The Andersen air sampler (Tokyo Direc Corporation AN-200) was installed on the upper deck. The wind vane and anemometer were installed with the air sampler to avoid contamination from the ship's exhaust; limited power was turned on when the headwind (120 deg; -60 to +60 deg relative to the bow) and with the wind speed greater than 3 m/s. The detailed sampling area is shown in Figure 3.3-9 and Table 3.3-8.

Chl-a, Cells Counting:

The samples were collected from the surface ocean (0 m, underway) with the pumping system. About 250 ml of sea water was collected for Chl-a samples with GF/F and membrane filter (pore size; 10 μm, 5 μm, 2 μm). About 500 ml of sea water was collected for Cells Counting with 0.45 μm membrane filters.

The detailed locations where Chl-a, Cell Count samples were collected are shown in Figure 3.3-9 and Table 3.3-9.

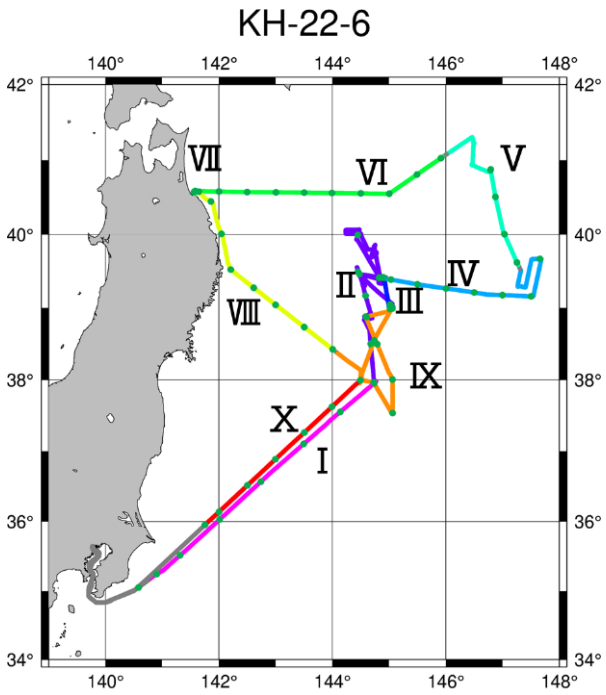

Figure 3.3-9. Sampling map

Table 3.3-8. Aerosol sampling location

Sampling Area	Start / Finish	Date (JST)			Time (JST)	Position					
Ⅰ	Start	2022	4	6	20:35	35° 1.7967	N	140° 32.9367	E
	Finish	2022	4	7	22:47	37° 57.8609	N	144° 43.4449	E
Ⅱ	Start	2022	4	7	23:11	37° 57.8605	N	144° 43.5722	E
	Finish	2022	4	12	9:15	38° 59.5207	N	145° 03.5074	E
Ⅲ	Start	2022	4	12	9:37	38° 59.5247	N	145° 03.5065	E
	Finish	2022	4	13	12:24	39° 24.9303	N	144° 52.8680	E
Ⅳ	Start	2022	4	13	13:16	39° 24.4429	N	144° 52.5224	E
	Finish	2022	4	14	4:45	39° 31.1310	N	147° 19.0647	E
Ⅴ	Start	2022	4	14	5:05	39° 35.3495	N	147° 16.3739	E
	Finish	2022	4	15	6:00	41° 05.2224	N	146° 01.9477	E
Ⅵ	Start	2022	4	15	6:19	41° 02.6631	N	145° 56.9119	E
	Finish	2022	4	15	19:21	40° 35.0807	N	141° 34.9941	E
Ⅶ	Start	2022	4	15	19:56	40° 35.1964	N	141° 34.8482	E
	Finish	2022	4	17	15:02	40° 34.2723	N	141° 33.8628	E
Ⅷ	Start	2022	4	17	16:10	40° 34.3808	N	141° 33.9170	E
	Finish	2022	4	18	5:33	38° 23.2831	N	144° 04.0266	E
Ⅸ	Start	2022	4	18	5:49	38° 20.6717	N	144° 08.2623	E
	Finish	2022	4	21	2:35	37° 59.7803	N	144° 29.3595	E
Ⅹ	Start	2022	4	21	3:00	37° 59.7472	N	144° 29.3739	E
	Finish	2022	4	21	16:51	35° 55.8824	N	141° 43.6201	E

Table 3.3-9. Chl-a, cells counting, biomarker sampling location

Sampling No.	Method	Date (JST)			Time (JST)	Position					
SO1	pump	2022	4	6	20:44	35	03.00	N	140	34.92	E
SO1a	pump				22:09	35	14.66	N	140	54.17	E
SO2	pump	2022	4	7	0:02	35	30.88	N	141	18.86	E
SO3	pump				3:13	36	01.76	N	142	00.66	E
SO4	pump				6:27	36	34.18	N	142	44.37	E
SO5	pump				9:36	37	06.25	N	143	29.67	E
SO6	pump				12:16	37	33.24	N	144	08.31	E
SO7	pump				15:51	37	57.27	N	144	44.36	E
SO8	pump	2022	4	8	2:04	38	30.16	N	144	40.53	E
SO9	pump				7:46	39	09.95	N	144	35.08	E
SO10	pump				13:33	39	29.65	N	144	27.02	E
SO11	pump				17:49	39	24.53	N	144	49.51	E
SO12	pump	2022	4	9	10:50	39	25.00	N	144	49.60	E
SO13	pump				16:09	39	59.58	N	144	26.87	E
SO14	pump	2022	4	10	9:19	39	24.99	N	144	53.73	E
SO15	pump	2022	4	11	11:59	39	27.65	N	144	28.72	E
SO15a	pump	2022	4	12	8:16	39	00.24	N	145	03.45	E
SO16	pump				10:25	38	59.39	N	145	03.50	E
SO16a	pump				17:54	39	02.66	N	145	01.03	E
SO16b	pump	2022	4	13	7:45	39	25.01	N	144	53.84	E
SO17	pump				10:50	39	24.72	N	144	53.73	E
SO17a	pump				13:50	39	23.15	N	145	01.92	E
SO18	pump				15:17	39	19.30	N	145	29.93	E
SO19	pump				16:51	39	15.89	N	146	00.19	E
SO20	pump				18:26	39	12.53	N	146	30.03	E
SO21	pump				19:58	39	10.44	N	146	59.91	E
SO22	pump				21:41	39	09.41	N	147	30.12	E
SO23	pump	2022	4	14	0:34	39	40.09	N	147	39.51	E
SO24	pump				5:13	39	37.20	N	147	15.24	E
SO25	pump				6:54	40	00.30	N	147	01.95	E
SO26	pump				9:00	40	30.42	N	146	52.47	E
SO26a	pump				12:21	40	52.01	N	146	47.21	E
SS26a	bucket				17:05	40	52.58	N	146	47.45	E
SO27	pump	2022	4	15	6:26	41	01.56	N	145	54.80	E
SO27a	pump				8:00	40	48.45	N	145	29.45	E
SO28	pump				9:50	40	33.00	N	145	00.13	E
SO29	pump				11:13	40	33.25	N	144	30.01	E
SO30	pump				12:38	40	33.54	N	143	59.60	E
SO30a	pump				13:57	40	33.85	N	143	30.24	E
SO31	pump				15:17	40	34.08	N	143	00.28	E
SO31a	pump				16:38	40	34.32	N	142	29.88	E
SO32	pump				18:07	40	34.71	N	142	00.03	E
SO33	pump				20:25	40	35.21	N	141	34.94	E
SO34	pump	2022	4	16	15:21	40	34.31	N	141	33.59	E
SO34a	pump				21:34	40	34.30	N	141	33.84	E
SO35	pump	2022	4	17	10:30	40	34.37	N	141	33.69	E
SO35a	pump				17:06	40	34.59	N	141	38.82	E
SO36	pump				18:34	40	26.75	N	141	51.55	E
SO37	pump				20:24	40	00.54	N	142	02.69	E
SO38	pump				22:18	39	31.36	N	142	12.47	E
SO38a	pump				23:51	39	16.41	N	142	36.83	E

SO39	pump	2022	4	18	1:21	39	02.41	N	142	59.94	E
SO39a	pump				3:20	38	44.00	N	143	30.22	E
SO40	pump				5:18	38	25.56	N	144	00.29	E
SO41	pump				11:01	38	32.99	N	144	44.30	E
SO42	pump				16:09	38	58.97	N	145	01.01	E
SO42a	pump	2022	4	19	6:45	38	52.36	N	144	36.03	E
SO43	pump				17:58	38	52.56	N	144	35.60	E
SO43a	pump				23:53	38	29.93	N	144	47.27	E
SO44	pump	2022	4	20	2:22	38	00.37	N	145	03.54	E
SO45	pump				5:06	37	32.23	N	145	03.69	E
SO45a	pump				11:10	37	58.07	N	144	43.70	E
SO46	pump				15:20	37	59.84	N	144	29.66	E
SO46a	pump	2022	4	21	6:12	37	37.53	N	143	59.52	E
SO47	pump				8:33	37	15.81	N	143	30.28	E
SO47a	pump				11:01	36	53.20	N	142	59.70	E
SO48	pump				13:08	36	31.01	N	142	30.14	E
SO48a	pump				15:33	36	08.33	N	142	00.09	E
SO49	pump				16:44	35	57.11	N	141	45.18	E

3) Anticipated results and future work plans

After disembarking from the cruise, the major components of the aerosol samples will be analyzed with ion chromatography, and REEs (aerosol samples) will be measured with ICP-MS (ELEMENT-II) using the isotope dilution method at the University of Toyama. The data will be analyzed and their influence on the surface ocean and seafloor sediment will be analyzed.

Chlorophyll-a will be measured by a Tuner Design Fluorometer, and the Cells Counting samples will be analyzed with a Scanning Electron Microscope at the University of Toyama.

The samples analyses are expected to be finished within one year after the cruise and the results will be submitted by middle 2024.

4. References

Ando, K., M. Kawabe, D. Yanagimoto, and S. Fujio (2013) Pathway and variability of deep circulation around 40°N in the northwest Pacific Ocean, *J. Oceanogr.*, **69**, 159-174.

Bristow, K.L., G.J. Kluitenberg, and R. Horton (1994) Measurement of soil thermal properties with a dual-probe heat-pulse technique, *Soil Sci. Soc. Am. J.*, **58**, 1288-1294.

Fujie, G., S. Kodaira, Y. Kaiho, Y. Yamamoto, T. Takahashi, S. Miura, and T. Yamada (2018) Controlling factor of incoming plate hydration at the north-western Pacific margin, *Nature Comm.*, **9**, 3844, doi:10.1038/s41467-018-06320-z.

Hirano, N., E. Takahashi, J. Yamamoto, N. Abe, S.P. Ingle, I. Kaneoka, T. Hirata, J.-I. Kimura, T, Ishii, Y. Ogawa, S. Machida, and K. Suyehiro (2006) Volcanism in response to plate flexure, *Science*, **313**, 1426-1428.

Kawada, Y., M. Yamano, and N. Seama (2014) Hydrothermal heat mining in an incoming oceanic plate due to aquifer thickening: Explaining the high heat flow anomaly observed around the Japan Trench, *Geochem. Geophys. Geosyst.*, **15**, 1580–1599, doi:10.1002/2014GC005285.

Park, J.-O., N. Takahata, E. Jamali Hondori, A. Yamaguchi, T. Kagoshima, T. Tsuru, G. Fujie, Y. Sun, J. Ashi, M. Yamano, Y. Sano (2021) Mantle-derived helium released through the Japan trench bend-faults, *Sci. Rep.*, **11**, 12026, doi:10.1038/s41598-021-91523-6.

Sass, J.H., C. Stone, and R.J. Munroe (1984) Thermal conductivity determinations on solid rocks - a comparison between a steady-state divided-bar apparatus and a commercial transient line-source device, *J. Volcanol. Geotherm. Res.*, **20**, 145-153.

Yamano, M., H. Hamamoto, Y. Kawada, and S. Goto (2014) Heat flow anomaly on the seaward side of the Japan Trench associated with deformation of the incoming Pacific plate, *Earth Planet. Sci. Lett.*, **407**, 196-204.

Von Herzen, R. and A.E. Maxwell (1959) The measurement of thermal conductivity of deep-sea sediments by a needle-probe method, *J. Geophys. Res.*, **64**, 1557-1563.

Notice on Using

This cruise report is a preliminary documentation as of the end of cruise.

This report is not necessarily corrected even if there is any inaccurate description (i.e. taxonomic classifications). This report is subject to be revised without notice. Some data on this report may be raw or unprocessed. If you are going to use or refer the data on this report, it is recommended to ask the Chief Scientist for latest status.

Users of information on this report are requested to submit Publication Report to Cooperative Research Cruise office.

E-mail: kyodoriyo@aori.u-tokyo.ac.jp